JOURNAL OF CATALYSIS 106, 85–92 (1987)

Quantitative Raman Characterization of Mo/TiO_2 Catalysts

ROGER B. QUINCY, MARWAN HOUALLA, AND DAVID M. HERCULES

Department of Chemistry, University of Pittsburgh, Pittsburgh, Pennsylvania

Received September 30, 1986; revised January 20, 1987

Two molybdenum species (i.e., Mo interaction species and MoO_3) are identified and quantitated by Raman spectroscopy for a series of Mo/TiO_2 catalysts. The Mo interaction species is shown to increase with Mo loading up to 6 wt% MoO_3 and to level off at higher Mo loadings. MoO_3 is detected at 7.5 wt% MoO_3/TiO_2 and shown to increase linearly with further Mo additions. The molybdenum speciation determined from Raman data is shown to correlate with ESCA and X-ray diffraction measurements. © 1987 Academic Press, Inc.

INTRODUCTION

Raman spectroscopy and X-ray photoelectron spectroscopy (XPS or ESCA) are complementary techniques that are used extensively to characterize supported molybdenum oxide catalysts. Whereas ESCA is valuable for determining molybdenum dispersion on the support, studies of Mo/Al_2O_3 by Zingg *et al.* (*1*) and by Grimblot and Payen (*2*) have shown that ESCA binding energy values alone cannot be used to distinguish among the various molybdenum oxide species sometimes present on these catalysts (e.g., MoO_3, $Al_2(MoO_4)_3$, Mo interaction species). Brown and Makovsky (*3, 4*) showed, however, that these molybdenum oxide species could be identified by Raman spectroscopy. Many subsequent Raman studies of Mo/Al_2O_3 (*5–18*), Mo/SiO_2 (*7, 9, 18–20*), and Mo/TiO_2 (*18, 21, 22*) have appeared in the literature. However, most of these studies were qualitative in nature. Few investigations have employed Raman spectroscopy to quantitate the species typically found on supported molybdenum oxide catalysts (*9, 17*).

The major objective of this paper is to show the importance of Raman spectroscopy for quantitating the molybdenum species present on Mo/TiO_2 catalysts. The Mo/TiO_2 system is ideal for conducting a quantitative Raman study because TiO_2 has several Raman active modes, providing an internal reference for Mo intensities. Changes in the Raman peaks due to molybdenum species can therefore be assessed accurately. Previous quantitative Raman studies of supported metal oxide catalysts have either relied on absolute peak intensity measurements (*23–27*), for which constant laser power is a necessity for all samples, or have introduced a Raman active material as an internal reference (*9, 17*). In addition, the present paper will show that the speciation determined from Raman data is supported by ESCA and X-ray diffraction (XRD) measurements.

EXPERIMENTAL

Catalyst Preparation

Degussa TiO_2 (7 : 3 anatase/rutile, pore volume ~0.5 cm^3/g, BET surface area 54 m^2/g) was ground with mortar and pestle after moistening with deionized water and drying at 120°C for 8 h. The ground support was then sieved to 100 mesh and calcined at 400°C for 8 h before incipient wetness impregnation with ammonium heptamolybdate (Fisher Scientific) solutions. The resulting Mo/TiO_2 catalysts were then dried at 120°C for 16 h followed by calcination in air at 500°C for 16 h. The surface area values for the various Mo/TiO_2 catalysts were essentially constant and equal to the value measured for the TiO_2 carrier when cor-

0021-9517/87 $3.00

rected for the amount of deposited molybdenum. The nomenclature used for the catalysts is "MoX" where X represents the molybdenum loading calculated as wt% MoO_3. The Mo loadings range from 1 to 15 wt% MoO_3.

Spectral Data Acquisition

The Raman spectra were recorded on a Spex Ramalog spectrometer equipped with holographic gratings. The 5145-Å line from a spectra-Physics Model 165 argon-ion laser was adjusted so that ~50 mW of power was measured at the sample. The spectral slitwidth was 4 cm^{-1}, and the scan rate was 0.4 cm^{-1}/sec. A Spex Datamate computer was used for data analysis (peak positions and peak areas). The peak positions were reproducible to ±2 cm^{-1}, and the average reproducibility in peak area intensity ratios was ±7%. The peak areas were calculated assuming a linear background. For the Mo/TiO_2 catalysts which contained MoO_3, the 996-cm^{-1} MoO_3 peak sometimes interfered with the broad peak for the Mo interaction species. This interference was minimal for the catalysts scanned in air (i.e., ambient conditions), and the 996-cm^{-1} MoO_3 peak was easily subtracted from the peak due to the Mo interaction species. However, these peaks overlapped severely for the catalysts scanned *in situ* after O_2 calcination. Thus, the area due to the 996-cm^{-1} MoO_3 peak was calculated by multiplying the measured 996-cm^{-1}/820-cm^{-1} ratio (0.172) for pure MoO_3 by the measured area of the MoO_3 820-cm^{-1} peak for the catalysts. This calculated 996-cm^{-1} peak area was then subtracted from the total area (i.e., area of Mo interaction species plus MoO_3) to give the area due to the Mo interaction species.

The catalysts scanned under ambient conditions were pressed into 13-mm-diameter KBr-backed pellets and rotated. *In situ* analyses were carried out in a sample cell containing a quartz optical flat. The catalysts were pressed into 13-mm-diameter pellets without backing and attached to a rotary feedthrough within the sample cell. The sample cell was attached to stainless steel vacuum components and could be evacuated with a turbomolecular pump, flushed with selected gases, heated in a tubular furnace, and positioned at the entrance optics of the Spex Ramalog spectrometer (*15*).

In situ spectra were obtained after the following treatment. The catalysts were evacuated to ~1 mTorr while being heated to 400°C (average heating rate 6°C/min). Dry oxygen (~760 Torr) was then slowly leaked into the cell which enclosed the heated catalysts. After ~30 min the sample cell was again evacuated and subsequently backfilled with dry oxygen. The catalysts were allowed to sit under these conditions for ~16 h. The following morning evacuation and backfilling was again repeated. After treating with the new dose of O_2 at 400°C for an hour, the catalysts were cooled to room temperature before spectral data acquisition.

A Diano diffractometer equipped with a graphite monochromator and a copper X-ray tube was used for XRD data. The X-ray tube was operated at 50 kV and 25 mA, and the scan rate was 0.4 deg/min (in 2θ deg). The powdered samples were packed into a 2 × 2 × 0.2-cm^3 hollowed-out plastic slide for analysis. Peak areas were measured with a planimeter and the average reproducibility for a measurement was ±5%.

ESCA spectra were obtained with an AEI ES200A electron spectrometer equipped with an aluminum anode (Al $K\alpha$ = 1486.6 eV). The anode was operated at 12 kV and 22 mA; the base pressure of the spectrometer was ~5×10^{-8} Torr. The catalysts were analyzed as powders dusted on sticky tape. The spectrometer was interfaced to an AEI DS100 data system for acquisition of spectra. The digital data were processed with an Apple II plus computer for measuring peak areas. At least three determinations were obtained for each catalyst, and the average reproducibility in peak area intensity ratios was ±3%. ESCA peak area intensity ratios ($I_{metal}/I_{support}$)

were used to monitor the extent of metal dispersion on the TiO_2 support.

RESULTS AND DISCUSSION

Figure 1a shows the Raman spectrum for Degussa TiO_2. The peaks observed at 197, 396, 516, and 638 cm^{-1} are due to the anatase form of TiO_2, while the 448-cm^{-1} peak is indicative of the rutile phase. The weak band at ~800 cm^{-1} has been assigned to the first overtone of the 396-cm^{-1} anatase mode (*28*). Figure 1b shows the Raman spectrum of the Mo4 catalyst scanned under ambient conditions. The broad peak centered at ~960 cm^{-1} has been attributed to a Mo=O stretching mode (*15, 21*) of a surface molybdate species (*15, 22*) or Mo interaction species (*1*). Figure 1c shows that *in situ* calcination (400°C, 16 h) of the Mo4 catalyst results in the narrowing of the peak due to the Mo interaction species and a shift in its position to 1002 cm^{-1}. The Raman peak positions of the Mo interaction species obtained for catalysts scanned under both ambient and *in situ* conditions are listed in Table 1. Note that for catalysts scanned under ambient conditions the peak position of the Mo interaction species increases in frequency from 942 cm^{-1} for the Mo1 catalyst to an average value of 962.5 ± 1.4 cm^{-1} for catalysts with Mo loadings ≥4 wt% MoO_3. This dependence of peak position on Mo loading for the Mo interaction species is in good agreement with previous Raman results obtained under ambient conditions for Mo/TiO_2 (*21, 22*) and Mo/Al_2O_3 catalysts (*7, 9–11, 15*). Recent *in situ* Raman investigations (*15, 16, 29*) have demonstrated that the position of this band is affected by moisture, and the band shift with Mo coverage has thus been attributed to the extent of hydration of the surface molybdate species which is coverage dependent (*29*). Table 1 shows that after *in situ* calcination the position of the peak for the Mo interaction species shifts to a constant value (1000 ± 1 cm^{-1}) for all of the catalysts. The position of the Mo interaction species after *in situ* calcination is consistent with the reported value for a 12 wt% MoO_3/TiO_2 catalyst (*30*). This shift in peak position to higher frequencies after *in situ* calcination has also been reported for similar

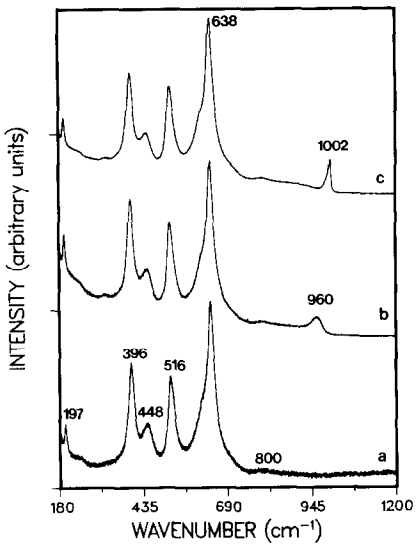

FIG. 1. Raman spectra of TiO_2 and a 4 wt% MoO_3/TiO_2 catalyst after various treatments. (a) Degussa TiO_2, (b) Mo4 scanned under ambient conditions, (c) Mo4 scanned in the Raman cell after 16 h 400°C O_2 calcination.

TABLE 1

Peak Position of Mo Interaction Species Observed by Raman Spectroscopy

Catalyst:	*Mo*1	*Mo*2	*Mo*4	*Mo*6	*Mo*7.5	*Mo*9	*Mo*12	*Mo*15
Ambient[a]:	942	948	961 ± 0.8	962	963 ± 1.2	961	964	964 ± 0.2
In situ[b]:	1000	1001	1002	1002	—	~1000[c]	~1002[c]	~1000[c]

[a] Catalyst pressed into a KBr backed pellet and scanned under ambient conditions.

[b] Catalyst pressed without backing and scanned in the Raman cell after ~16 h O_2 400°C calcination.

[c] Mo interaction species peak position has been approximated because of interference due to the MoO_3 peak at 996 cm^{-1}.

supported metal oxide systems: Mo/Al_2O_3 (*15, 16, 29*), W/Al_2O_3 (*29, 31*), Re/Al_2O_3 (*32*), V/Al_2O_3 (*29*), and W/TiO_2 (*29*), and has been attributed to an increase in the terminal M=O bond order, resulting from the desorption of H_2O (*15, 16, 29, 31*).

Figure 2 shows the Raman spectra obtained under ambient conditions for four Mo/TiO_2 catalysts. Note that catalysts having molybdenum loadings below 7.5 wt% MoO_3 show only the Raman band characteristic of Mo interaction species (Figs. 2a and 2b). The Raman spectra of catalysts with Mo loadings of 7.5 wt% MoO_3 or greater also show the presence of MoO_3 (e.g., peaks at 288, 338, 820, and 996 cm^{-1} in Figs. 2c and 2d). A plot of the Mo interaction species/TiO_2 anatase 516-cm^{-1} Raman peak area ratio as a function of molybdenum loading is shown in Fig. 3 for catalysts scanned under both ambient and *in situ* conditions. The intensity ratio values are seen to differ for the two cases, particularly for the 6 wt% MoO_3/TiO_2 and 9 wt% MoO_3/TiO_2 catalysts. This difference may be due to a change in the Raman scattering cross section of the Mo interaction species after dehydration. The dependence of the intensity of the Mo interaction species on the condition of the catalyst (i.e., state of hydration) has also been reported for Mo/Al_2O_3 catalysts (*4*). The important point to note in Fig. 3 is that the intensity of Mo interaction species follows the same trend for both the ambient and *in situ* cases; it increases with Mo loading up to ~6 wt% MoO_3 and levels off at higher Mo loadings. Figure 4 shows a plot of the MoO_3 820-cm^{-1}/TiO_2 anatase 516-cm^{-1} Raman peak

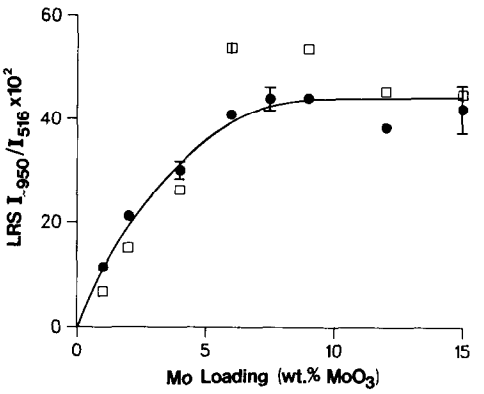

FIG. 3. Plot of the Raman peak area intensity ratio of the Mo interaction species/TiO_2 anatase 516-cm^{-1} vs Mo loading for Mo/TiO_2 catalysts. (●) catalysts scanned under ambient conditions, (□) catalysts scanned *in situ* after 16 h 400°C O_2 calcination (I = standard deviation, | = the spread from the mean for two replications).

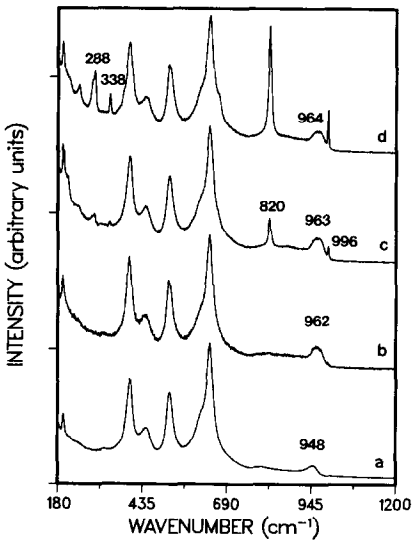

FIG. 2. Raman spectra of four Mo/TiO_2 catalysts scanned under ambient conditions. (a) Mo2, (b) Mo6, (c) Mo7.5, (d) Mo12.

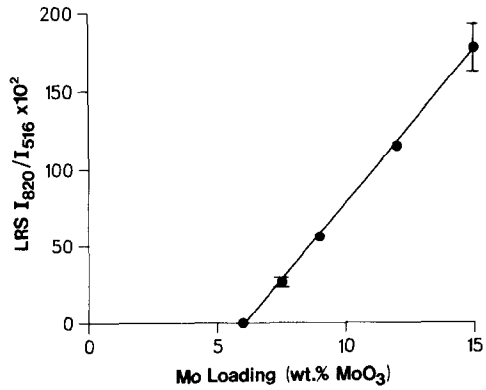

FIG. 4. Plot of the Raman area intensity ratio of MoO_3/TiO_2 anatase (I_{820}/I_{516}) for Mo/TiO_2 catalysts. Catalysts were scanned under ambient conditions (I = standard deviation).

area ratios vs Mo loading for the Mo/TiO_2 catalysts scanned under ambient conditions. MoO_3 is first observed for the Mo7.5 catalyst and increases linearly with further Mo addition. The MoO_3 820-cm^{-1}/TiO_2 anatase 516-cm^{-1} peak area ratios vs Mo loading also exhibit linear behavior when plotted for catalysts scanned after *in situ* calcination. However, an increase in the intensities of both the MoO_3 and TiO_2 bands is observed after catalyst dehydration. This effect is more pronounced for the MoO_3 820-cm^{-1} band, and is illustrated by approximately 50% higher MoO_3 820-cm^{-1}/TiO_2 anatase 516-cm^{-1} intensity ratios for catalysts scanned after *in situ* calcination.

To estimate the amount of MoO_3 present, a calibration curve was constructed by plotting the MoO_3 820-cm^{-1}/TiO_2 anatase 516-cm^{-1} peak area ratios as a function of wt% MoO_3 for various MoO_3/TiO_2 physical mixtures, as shown in Fig. 5. The physical mixtures were scanned under ambient conditions. Linearity is observed up to 12 wt% MoO_3; the correlation coefficient is 0.997, the slope is 0.223, and the intercept is 0.00112. The calibration curve was used to calculate the MoO_3 content for the catalysts scanned under ambient conditions. The amount of molybdenum present as the Mo interaction species was determined by subtracting the absolute amount of MoO_3

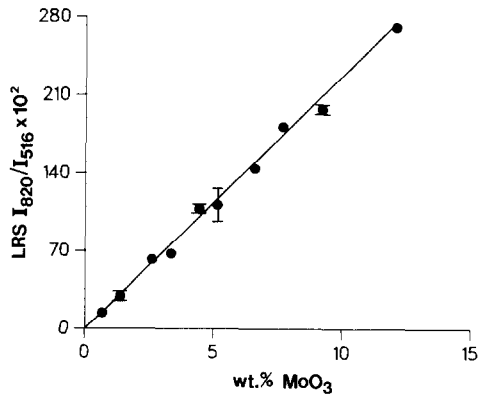

FIG. 5. Raman calibration curve for MoO_3/TiO_2 physical mixtures. The physical mixtures were scanned under ambient conditions (I = standard deviation).

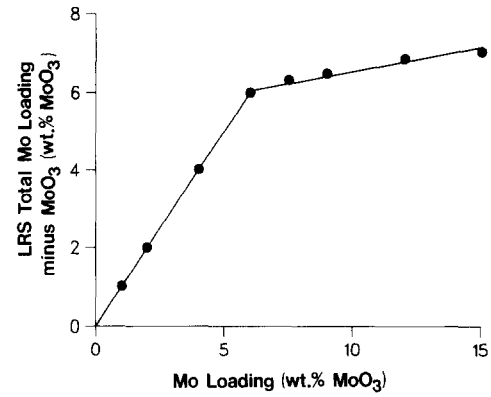

FIG. 6. Total Mo loading minus MoO_3 (i.e., calculated amount of Mo interaction species) for Mo/TiO_2 catalysts scanned under ambient conditions. The amount of Mo interaction species is expressed in terms of wt% MoO_3.

present in the Mo7.5 to Mo15 catalysts from the total Mo loading. The results are plotted in Fig. 6 as a function of Mo content. It can be readily seen that the calculated variation in the amount of Mo interaction species (Fig. 6) agrees with the observed changes of the Raman peaks characteristic of Mo interaction species as function of Mo loading (Fig. 3).

From the quantity of Mo interaction species and MoO_3 present on the Mo/TiO_2 catalysts, it is possible to calculate their relative Raman scattering cross sections. The average relative cross section of MoO_3 to that of the Mo interaction species is 3.6 (±0.4). Baltrus *et al.* (*17*) calculated for a series of Mo/Al_2O_3 catalysts an average MoO_3 to Mo interaction species relative Raman cross section of 17 : 1. This suggests that the Mo : TiO_2 interaction species has a larger Raman scattering cross section than the corresponding Mo : Al_2O_3 surface phase.

X-ray diffraction was employed to follow the variation of the amount of crystalline MoO_3 as a function of molybdenum loading for the Mo/TiO_2 catalysts. The XRD patterns for catalysts having molybdenum loadings below 7.5 wt% MoO_3 show only peaks characteristic of the anatase and rutile forms of TiO_2. Two additional weak

peaks at 2θ = 23.3 and 49.2 in the XRD pattern are easily detected for catalysts with higher molybdenum loadings (e.g., Mo9–Mo15). Figure 7 shows the variation of the MoO_3 (110)/TiO_2 rutile (111) peak area intensity ratios for these catalysts (i.e., Mo9, Mo12, and Mo15) and for a series of MoO_3/TiO_2 physical mixtures. The MoO_3/TiO_2 calibration curve (Fig. 7) was used to estimate the amount of crystalline MoO_3 present for the Mo9–Mo15 catalysts. The Mo9, Mo12, Mo15 catalysts were found to contain 3.1, 6.2, and 8.8 wt% crystalline MoO_3, respectively, as illustrated in Figure 7. Thus, after subtracting the amount of crystalline MoO_3 from the total molybdenum content for each catalyst (i.e., Mo9, Mo12, Mo15), approximately 6 wt% MoO_3 remains unaccountable by XRD. This is consistent with the Raman results; catalysts with Mo loadings ≤6 wt% MoO_3 contain only Mo interaction species while catalysts with Mo loadings >6 wt% MoO_3 contain essentially constant amounts of Mo interaction species (i.e., ~6 wt% MoO_3) but increasing amounts of MoO_3. The agreement between the Raman and XRD results also indicates that most of the MoO_3 formed is crystalline.

ESCA was used to monitor the dispersion of molybdenum on the TiO_2 support. Figure 8 shows the ESCA Mo 3d/Ti 2*p* peak

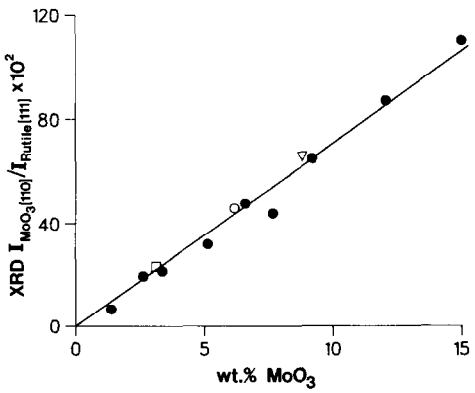

FIG. 7. XRD MoO_3 (110)/TiO_2 rutile (111) peak area intensity ratios vs amount of MoO_3 (wt% MoO_3) for MoO_3/TiO_2 physical mixtures (●) and for Mo9 (□), Mo12 (○), and Mo15 (△) catalysts.

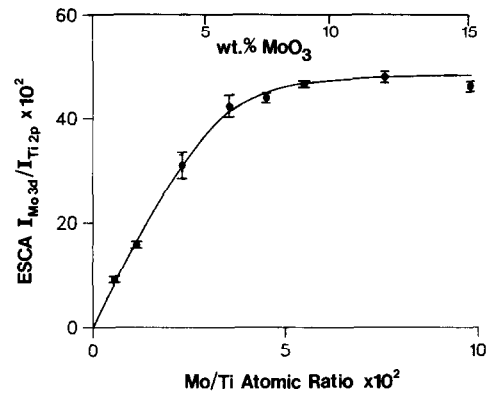

FIG. 8. ESCA Mo 3d/Ti 2*p* peak area intensity ratios vs Mo loading for Mo/TiO_2 catalysts (I = standard deviation).

area intensity ratios as a function of molybdenum loading. It can be seen that the Mo 3d/Ti 2*p* peak area ratios increase linearly up to 6 wt% MoO_3 and level off for further Mo additions. It is worth noting the similarity between the ESCA Mo/Ti intensity ratios (Fig. 8) and the evolution of the Raman peak attributed to Mo interaction species (Fig. 3) as a function of molybdenum loading. The linear increase of the ESCA Mo/Ti intensity ratios with increasing Mo loading up to 6 wt% MoO_3 is indicative of a uniformly dispersed Mo phase; this is consistent with the presence of Mo interaction species. Furthermore, the break in the ESCA curve and leveling off after 6 wt% MoO_3 corresponds to a significant decrease in Mo dispersion. This is consistent with the Raman and XRD results which show that catalysts with Mo loadings >6 wt% MoO_3 contain essentially constant amounts of Mo interaction species but increasing amounts of MoO_3.

This paper has demonstrated the importance of Raman spectroscopy for quantitating the molybdenum species present on Mo/TiO_2 catalysts. It must be noted, however, that the Mo/TiO_2 catalyst series presents an ideal system for conducting a quantitative Raman study for two reasons. First, as mentioned previously, the support provides an internal reference, and second,

only slight color changes occur as the Mo loading is increased. Changes in the color of a catalyst as the metal loading is varied may indeed preclude the use of Raman spectroscopy for quantitative analysis (*33*).

CONCLUSION

The molybdenum speciation (i.e., quantity of Mo interaction species and MoO_3) was determined for a series of Mo/TiO_2 catalysts. The Mo interaction species was shown to increase with Mo loading up to 6 wt% MoO_3 and to level off at higher Mo loadings. MoO_3 was detected at a Mo loading of 7.5 wt% MoO_3 and shown to increase linearly with further molybdenum additions.

X-ray diffraction data provided an independent determination of the quantity of MoO_3 present for the Mo/TiO_2 catalysts. Agreement between the XRD and Raman measurements indicated that most of the MoO_3 formed is crystalline.

The ESCA data were shown to correlate with the Raman and XRD results. Specifically, a Mo phase of uniform dispersion was observed for Mo loadings $\leq$6 wt% MoO_3, and a decrease in molybdenum dispersion, consistent with MoO_3 formation, was found for higher Mo loadings.

ACKNOWLEDGMENTS

We gratefully acknowledge Dennis Finseth and Leo Makovsky from the Department of Energy's Pittsburgh Energy Technology Center (PETC) for stimulating discussion and for use of the Raman spectrometer. We also thank Joe D'Este from PETC for assistance with the *in situ* Raman work. This work was supported by the Department of Energy under Grant No. DE-AC02-79ER10485. R. B. Quincy acknowledges the Gulf Oil Corporation and the A. W. Mellon Educational and Charitable Trust for Predoctoral Fellowships.

REFERENCES

1. Zingg, D. S., Makovsky, L. E., Tischer, R. E., Brown, F. R., and Hercules, D. M., *J. Phys. Chem.* **84,** 2898 (1980).
2. Grimblot, J., and Payen, E., *in* "Surface Properties and Catalysis by Non-Metals" (J. P. Bonnelle *et al.*, Eds.), p. 189. Reidel, Dordrecht, 1983.
3. Brown, F. R., and Makovsky, L. E., *Appl. Spectrosc.* **31,** 44 (1977).
4. Brown, F. R., Makovsky, L. E., and Rhee, K. H., *J. Catal.* **50,** 162 (1977).
5. Medema, J., van Stam, C., de Beer, V. H. J., Konings, A. J. A., and Koningsberger, D. C., *J. Catal.* **53,** 386 (1978).
6. Jeziorowski, H., and Knozinger, H., *J. Phys. Chem.* **83,** 1166 (1979).
7. Cheng, C. P., and Schrader, G. L., *J. Catal.* **60,** 276 (1979).
8. Iannibello, A., Marengo, S., and Villa, P. L., "Proc. Third Int. Conf. on the Chemistry and Uses of Molybdenum" (P. C. H. Mitchell and H. F. Barry, Eds.), p. 92. Climax Molybdenum Company, Ann Arbor, MI, 1979.
9. Thomas, R., Mittelmeijer-Hazeleger, M. C., Kerkhof, F. P. J. M., Moulijn, J. A., Medema, J., and de Beer, V. H. J., "Proc. Third Int. Conf. on the Chemistry and Uses of Molybdenum" (P. C. H. Mitchell and H. F. Barry, Eds.), p. 85. Climax Molybdenum Company, Ann Arbor, MI, 1979.
10. Wang, L., and Hall, W. K., *J. Catal.* **66,** 251 (1980).
11. Sombret, B., Dhamelincourt, P., Wallart, F., Muller, A. C., Bouquet, M., and Grosmangin, J., *J. Raman Spectrosc.* **9,** 291 (1980).
12. Dufresne, P., Payen, E., Grimblot, J., and Bonnelle, J. P., *J. Phys. Chem.* **85,** 2344 (1981).
13. Lopez Agudo, A., Gil, F. J., Calleja, J. M., and Fernandez, V., *J. Raman Spectrosc.* **11,** 454 (1981).
14. Kasztelan, S., Grimblot, J., Bonnelle, J. P., Payen, E., Toulhoat, H. and Jacquin, Y., *Appl. Catal.* **7,** 91 (1983).
15. Stencel, J. M., Makovsky, L. E., Sarkus, T. A., De Vries, J., Thomas, R., and Moulijn, J. A., *J. Catal.* **90,** 314 (1984).
16. Stencel, J. M., Makovsky, L. E., Diehl, J. R., and Sarkus, T. A., *J. Catal.* **95,** 414 (1985).
17. Baltrus, J. P., Makovsky, L. E., Stencel, J. M., and Hercules, D. M., *Anal. Chem.* **57,** 2500 (1985).
18. Leyrer, J., Vielhaber, B., Zaki, M. I., Shuxian, Z., Weitkamp, J., and Knozinger, H., *Mater. Chem. Phys.* **13,** 301 (1985).
19. Jeziorowski, H., Knozinger, H., Grange, P., and Gajardo, P., *J. Phys. Chem.* **84,** 1825 (1980).
20. Rodrigo, L., Marcinkowska, K., Adnot, A., Roberge, P. C., Kaliaguine, S., Stencel, J. M., Makovsky, L. E., and Diehl, J. R., *J. Phys. Chem.* **90,** 2690 (1986).
21. Ng, K. Y. S., and Gulari, E., *J. Catal.* **92,** 340 (1985).
22. Liu, Y. C., Griffin, G. L., Chan, S. S., and Wachs, I. E., *J. Catal.* **94,** 108 (1985).
23. Kerkhof, F. P. J. M., Moulijn, J. A., Thomas, R.,

and Oudejans, J. C., *in* "Preparation of Catalysts," Vol. II, "Scientific Basis for the Preparation of Heterogeneous Catalysts" (B. De! Grange, P. Jacobs, and G. Poncelet, Eds.), p. 77. Elsevier, Amsterdam, 1979.

24. Chan, S. S., Wachs, I. E., and Murrell, L. L., *J. Catal.* **90,** 150 (1984).
25. Chan, S. S., Wachs, I. E., Murrell, L. L., and Dispenziere, N. C., Jr., *J. Catal.* **92,** 1 (1985).
26. Saleh, R. Y., Wachs, I. E., Chan, S. S., and Claudio, C. C., *J. Catal.* **98,** 102 (1986).
27. Bond, G. C., Zurita, J. P., Flamerz, S., Gellings, P. J., Bosch, H., van Ommen, J. G., and Kip, B. J., *Appl. Catal.* **22,** 361 (1986).
28. Balachandran, U., and Eror, N. G., *J. Solid State Chem.* **42,** 276 (1982).
29. Chan, S. S., Wachs, I. E., Murrell, L. L., Wang, L., and Hall, W. K., *J. Phys. Chem.* **88,** 5831 (1984).
30. Wang, L., Ph.D. thesis, The University of Wisconsin–Milwaukee, 1982.
31. Stencel, J. M., Makovsky, L. E. Diehl, J. R., and Sarkus, T. A., *J. Raman Spectrosc.* **15,** 282 (1984).
32. Wang, L., and Hall, W. K., *J. Catal.* **82,** 177 (1983).
33. Quincy, R. B., Houalla, M., and Hercules, D. M., unpublished results.